Germylene Reactions with Quinones Shed Light on Germylene Phenone Equilibria

Ryan D. Sweeder, Robyn L. Gdula, Bonnie J. Ludwig, Mark M. Banaszak Holl,* and Jeff W. Kampf

Chemistry Department, University of Michigan, Ann Arbor, Michigan 48109-1055

Received April 9, 2003

$Ge[CH(SiMe_3)_2]_2$ (**1**) and $Ge[N(SiMe_3)_2]_2$ (**2**) react with anthraquinone and naphthoquinone in a 2:1 ratio to form five-membered rings with the carbonyl oxygens and the *ortho* carbons of the adjacent aromatic ring. The reaction with 1,4-diacetylbenzene proceeds in a similar fashion with **1**; however no reaction is observed with **2**. Compounds **1** and **2** react with 1,2-diacetylbenzene to yield a novel bicyclo species. In a previous report describing equilibria between **1** and phenones, it appeared that **2** did not undergo reaction to generate the five-membered ring with the accompanying formation of a conjugated triene. However, these quinone results indicate that an equilibrium can exist between **2** and a phenone moiety. In the reaction with quinones, a second equivalent of germylene effectively traps the conjugated triene by undergoing a 1,4-addition reaction. Unlike the initial triene formation, this second insertion is irreversible.

Introduction

Germylenes, divalent heavy metal analogues of carbenes, show a striking array of reactivity.[1−5] This reactivity is due in part to the presence of a Lewis acidic and a Lewis basic site on the same atom, allowing sequential electrophillic and nucleophilic bond-forming reactions. The Satgé group and others pioneered the arena of germylene reactivity with small organic molecules.[6,7] The facile kinetic reversibility of Ge−O, Ge−C, and Ge−H bonds[8−10] suggests that germanium could serve as an ideal activation agent and leaving group for synthetic organic applications. Two potentially useful germanium species are $Ge[CH(SiMe_3)_2]_2$ (**1**)[11] and $Ge[N(SiMe_3)_2]_2$ (**2**).[12] These compounds, prepared by Lappert et al., are convenient, stable, crystalline reagents that can be stored indefinitely under air-free conditions.

Reactions of germylenes with some diketones have been previously reported. α-Diketones, including *ortho* quinones, undergo a [1 + 4] cyclization reaction with germylenes.[10,13,14] This reaction allows α-diketones to be effective germylene traps. The reaction of germylenes with *para* quinones gives polymer.[15−17] A number of sterically stabilized germylenes were reported to react with *para* quinones to yield an alternating 2:1 polymer. An exception was noted for **2**, which yielded a 1:1 polymer upon reaction with a number of 1,4-quinones including naphthoquinone.

In a previous study, we reported that **1** reacted with a variety of phenone moieties to form conjugated triene species.[18] This facile, quantitative reaction is reversible, with the equilibrium heavily favoring the triene product. However, **2** was not observed to undergo the parallel reaction. It appeared that the additional stabilization of the germylene provided by the amide ligand was enough to inhibit triene formation.

In this study of the reactions of **1** and **2** with quinones and diacetyl benzenes, a better understanding of the dynamic relationship between germylenes and phenones is elucidated. The equilibria present between **1** and phenones does indeed lie heavily toward the formation of the conjugated triene. In the case of **2**, the ultimate reaction products indicate the same equilibrium exists; however the favored species are unreacted **2** and phenone.

Results and Discussion

Anthraquinone and Naphthoquinone. Both **1** and **2** react with anthraquinone in a 2:1 ratio to yield products **3** and **4**, respectively (Scheme 1). Both compounds feature two new five-membered rings and form

* Corresponding author.

(1) Lappert, M. F.; Rowe, R. S. *Coord. Chem. Rev.* **1990**, *100*, 267−292.
(2) Petz, W. *Chem. Rev.* **1986**, *86*, 1019−1047.
(3) Lappert, M. F. *Main Group Met. Chem.* **1994**, *17*, 183.
(4) Tokitoh, N.; Matsuhashi, Y.; Shibata, K.; Matsumoto, T.; Suzuki, H.; Saito, M.; Manmaru, K.; Okazaki, R. *Main Group Met. Chem.* **1994**, *17*, 55.
(5) Tandura, S. N.; Gurkova, S. N.; Gusev, A. I. *Zh. Strukt. Khim.* **1990**, *31*, 154.
(6) Satgé, J.; Massol, M.; Rivière, P. *J. Organomet. Chem.* **1973**, *56*, 1−39.
(7) Satgé, J. *J. Organomet. Chem.* **1990**, *400*, 121−147.
(8) Litz, K. E.; Kampf, J. W.; Banaszak Holl, M. M. *J. Am. Chem. Soc.* **1998**, *120*, 7484−7492.
(9) Litz, K. E.; Henderson, K.; Gourley, R. W.; Banaszak Holl, M. M. *Organometallics* **1995**, *14*, 5008−5010.
(10) Litz, K. E.; Bender, J. E.; Sweeder, R. D.; Banaszak Holl, M. M.; Kampf, J. W. *Organometallics* **2000**, *19*, 1186−1189.
(11) Fjeldberg, T.; Haaland, A.; Schilling, B. E. R.; Lappert, M. F.; Thorne, A. J. *J. Chem. Soc., Dalton Trans.* **1986**, 1551−1556.
(12) Gynane, M. J. S.; Harris, D. H.; Lappert, M. F.; Power, P. P.; Rivière, P.; Rivière-Baudet, M. *J. Chem. Soc., Dalton Trans.* **1977**, 2004−2009.
(13) Michels, E.; Neumann, W. P. *Tetrahedron Lett.* **1986**, *27*, 2455−2458.
(14) Satgé, J. *Chem. Heterocycl. Compd.* **2000**, *35*, 1013−1032.
(15) Kobayashi, S.; Iwata, S.; Abe, M.; Shoda, S. *J. Am. Chem. Soc.* **1990**, *112*, 1625−1626.
(16) Kobayashi, S.; Iwata, S.; Hiraishi, M. *J. Am. Chem. Soc.* **1994**, *116*, 6047−6048.
(17) Kobayashi, S.; Shoda, S. I.; Cao, S.; Iwata, S.; Abe, M.; Yajima, K.; Yagi, K.; Hiraishi, M. *J. Macromol. Sci.-Pure Appl. Chem.* **1994**, *A31*, 1835−1845.
(18) Sweeder, R. D.; Miller, K. A.; Banaszak Holl, M. M.; Kampf, J. W. *Organometallics* **2002**, *21*, 457−459.

10.1021/om0302589 CCC: $25.00
Publication on Web 06/28/2003

Scheme 1. Reactions of 1 and 2 with Diketones

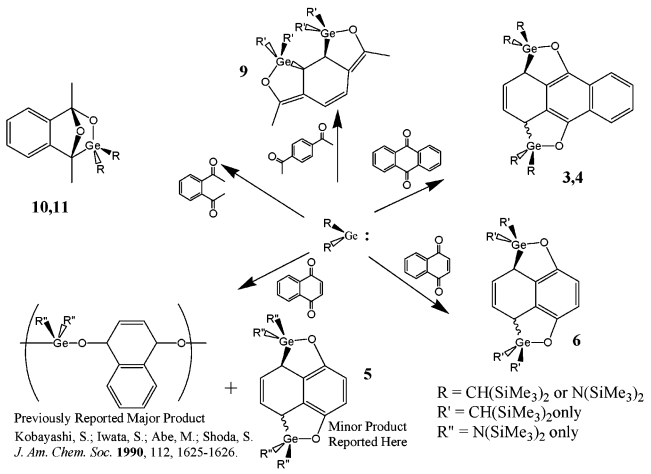

in many organic solvents including hexane, THF, benzene, toluene, and diethyl ether. Two isomers, believed to be the cisoid and transoid forms of the compound, are formed in a ~3:2 ratio as determined by NMR spectroscopy. Due to the chemical similarities of the two isomers, attempts at separation using sublimation, chromatography, or recrystallization have not been successful. Compound **3** is both air and water stable; however **4** is susceptible to hydrolysis of the Ge−N bonds.

Compounds **3** and **4** have proven to be robust species that do not undergo elimination of germylene as previously observed for phenone activations.[18] Instead, these compounds are stable in the presence of the known germylene trap, benzil,[10] even at elevated temperatures. Also, unlike previous phenone activation products,[18] **3** survives the presence of water and ethanol. These results indicate that an equilibrium with free quinone and germylene is not present in either case.

Quinones such as 1,4-naphthoquinone and *p*-benzoquinone have been previously reported to react with **2** and other germylenes to form alternating germanium quinone polymers in high yield.[15] We observed reaction between germylene **2** and 1,4-naphthoquinone to follow the literature results and produce polymer; however a small impurity with ^{1}H NMR spectroscopic chemical shifts consistent with the expected shifts for **5** (Scheme 1) was observed. Moderate yields (~50%) of **5** could be obtained through the slow addition of quinone solution to a solution of germylene at room temperature. The more sterically hindered **1** reacts readily with 1,4-naphthoquinone in a 2:1 ratio to yield **6** with no polymer formation.

A crystal of **6** was obtained by slow evaporation of a benzene solution at 25 °C. Single-crystal X-ray structure determination verified the general connectivity including both six-membered and five-membered rings (Figure 1). The ring containing C1 has been converted into an aromatic ring, as confirmed by the C−C distances: C1−C2 1.383(3); C2−C2A 1.403(4); C1−C3 1.390(3); C3−C3A 1.373(4) Å. The ring containing C4, which is the aromatic ring in the naphthoquinone starting material, is no longer aromatic, retaining only one double bond as confirmed by the following C−C distances: C3−C4 1.508(3); C4−C5 1.462(3); C5−C5A 1.368(5) Å. Although the crystal appears to contain only the *trans* isomer, ^{1}H NMR spectroscopy of the crystallized material still shows both isomers present. A small amount of disorder can be observed at C5, perhaps indicative of a cocrystallization of isomers similar to **3** (vide infra).

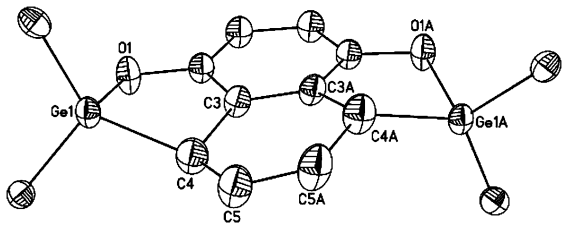

Figure 1. ORTEP of **6** with selected bond lengths (Å) and angles (deg): Ge(1)−O(1) 1.8612(15), Ge(1)−C(4) 2.003(2), C(4)−C(5) 1.462(3), C(5)−C(5A) 1.368(5), O(1)−Ge(1)−C(4) 89.12(8).

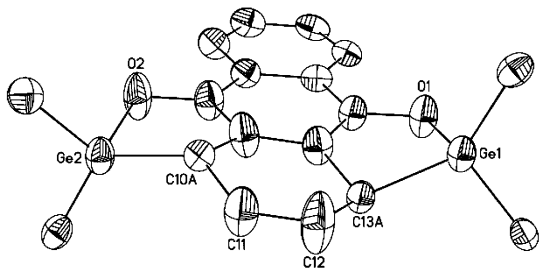

Figure 2. ORTEP of **3** with selected bond lengths (Å) and angles (deg). Only one resolved position at C(10) and C(13) shown: Ge(1)−O(1) 1.860(3), Ge(2)−O(2) 1.848(3), Ge(1)−C(13A) 2.002(3), Ge(2)−C(10A) 2.004(7), O(1)−Ge(1)−C(13A) 89.69(18), O(2)−Ge(2)−C(10A) 90.3(2).

A crystal of **3** was grown by slow evaporation of a pentane solution. A single crystal X-ray structure was obtained confirming the proposed connectivity (Figure 2); however C10, C11, C12, and C13 show considerable disorder that likely arises from the mixture of cisoid and transoid isomers present. The ^{1}H NMR spectrum of the same batch of single crystals suggests the ratio is 3:2. Molecular modeling studies indicate that the germylene ligands and two of the three rings can occupy a similar region of space for either the *cis* or *trans* isomers. Unfortunately, we were not successful in applying a crystallographic model to determine the relative percentage of *cis* and *trans* isomers in the crystal. The disorder in the structure prevents a meaningful metrical analysis of the ring system to which both germanium atoms are bound, and we can use the structure only to confirm the gross connectivity of the system.

A likely mechanism of formation for compounds **3**−**6** entails the addition of the first equivalent of germylene in a fashion identical to that previously reported for insertion into phenones (Scheme 2).[18] The second ketone is then prepared for a standard 1,4-addition of the germylene to a nonaromatic system in a manner consistent with earlier literature precedent.[13] The formation of both **4** and **5** is quite enlightening in that they demonstrate that the germylene **2** must be in equilibrium with the monoactivation product. This suggests **2** participates in an equilibrium with phenones to form the five-membered ring, even though the monoactivated product is not readily detectable via ^{1}H NMR or UV/vis spectroscopies.

A closer examination of the formation of **3** suggests that the germylene **1** more readily reacts with **7** than free anthraquinone. When the germylene and quinone

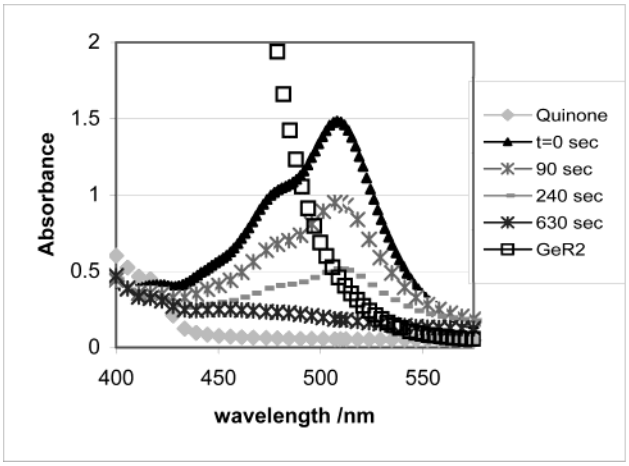

Figure 3. UV/vis after addition of **1** to anthraquinone.

Scheme 2. Addition of 1 to Anthraquinone

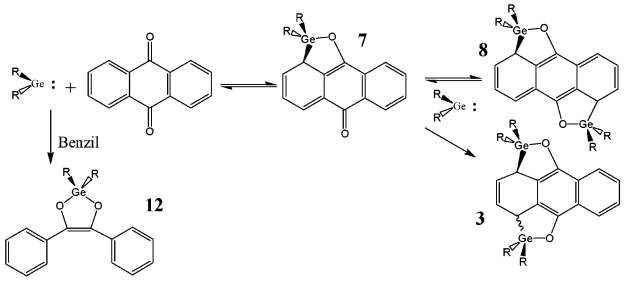

are mixed in a 1:1 ratio, all of **1** is consumed immediately, yielding UV/vis spectra indistinguishable from the 2:1 addition between 425 and 600 nm. However, an initial color change to deep red that slowly fades over a ~10 min period suggests a competing product (**8**) may be present (Figure 3). Free germylene **1** has an intense characteristic peak at 420 nm with an extinction coefficient of 2510 cm^{-1} M^{-1} that disappears immediately upon mixing with 0.5 equiv of anthraquinone. This indicates that the reaction mixture contains only species with a 2:1 ratio of germylene to anthraquinone such as **3** and **8**. The loss of the germylene-based absorption at 425 nm occurs simultaneously with the appearance of a new peak at 509 nm accompanied by shoulders at 480 and 450 nm. These peaks fade in unison until the color disappears and **3** is the only product present.

Although one could hypothesize that the resulting red color arises from intermediate **7**, this is inconsistent with the apparent reaction stoichiometry and the UV/vis spectroscopic data obtained (Figure 3). Geometry-optimized density functional theory calculations using the B3LYP functional and 6-31G* basis set indicate a HOMO−LUMO energy gap (π to π^* transition) of 2.72 eV for **7**, 2.43 eV for the *cis* isomer of **8**, and 2.48 eV for the *trans* isomer of **8**. These correspond to values of 456, 509, and 500 nm, respectively, as compared to the experimentally measured peak position of 509 nm. The excellent agreement for the calculated π to π^* transition of the *cis* isomer **8** combined with the previously mentioned stoichiometric arguments supports the assignment of **8** as a transient kinetic product present in this reaction. On the other hand, agreement with the experimentally measured value of 480 nm for either **7** (calcd 456 nm) or the *trans* isomer of **8** (calcd 500 nm) is poor. The *trans* isomer may be the source of the shoulder. The consistent relative ratio of this height to the main peak at 509 nm, even with varying the ratio of anthraquinone present from 0.5 equiv up to 2 equiv, is consistent with this assignment. The small shoulder at 450 nm may arise from a small amount of **7** present, very close to the predicted location of 456 nm.

To quantify the amount of **8** present in solution, a 7-fold excess of benzil was added to the solution immediately after UV/vis spectroscopy indicated all free germylene was consumed. Assuming that the reaction of excess benzil and germylene proceeds much faster than the reaction of **7** and **1** to yield **3**, a comparison of the concentrations of both **8** and **3** can be estimated at the time point when the benzil was added. It should be noted that the small amount of **7** will also result in trapped germylene.

Addition of a 7-fold excess of benzil 35 s after initiating the reaction resulted in the formation of 39% trapped product (**12**) and 61% **3** as quantified by ^{1}H NMR spectroscopy. Under the experimental conditions employed, this indicates a 0.86 mM concentration of **8** at the time of benzil addition. Assuming that Beer's law is effectively obeyed at this concentration, a molar absorptivity of $\epsilon = 1201$ cm^{-1} M^{-1} is calculated, a reasonable value for a $\pi \rightarrow \pi^*$ transition. This method would have also converted any **7** or free **1** present to **12** as well; thus the number obtained is effectively a lower bound for the molar absorptivity. Applying the molar absorptivity value to experiments in which the formation and disappearance of **8** was monitored every 35 s by UV/vis scans indicates an initial **8**:**3** ratio of 1.2:1. Thus, formation of **8** is competitive or slightly kinetically favored over **3**.

Both **3** and **8** are likely formed through **7** (the result of the initial reaction of **1** with anthraquinone.) This initial insertion to form **7** causes the loss of aromaticity in the quinone's fused benzene ring, forming a conjugated triene. The loss of aromaticity carries a high thermodynamic cost, partially negating the energy release from the formation of the new Ge−O and Ge−C bonds. Using standard bond energy tables one finds a net stabilization of 6 kcal/mol for the formation of **7**.[19,20] From **7**, two possible germylene insertions may occur. A second germylene insertion may occur on the remaining aromatic ring, leading to **8**. This second insertion would be expected to have a similar thermodynamic profile, suggesting another 6 kcal/mol stabilization. A second germylene may instead insert into the activated ring of **7** to form **3** without the energy cost required to break the aromaticity. Further, the formation of **3** actually induces aromaticity on the middle six-membered ring. Standard tables estimate the second insertion to form **3** to be favorable by 42 kcal/mol. This strong thermodynamic driving force appears to be the difference between the reversible formation of **8** and the nonreversibility of the formation of **3**. DFT molecular modeling calculations with the 6-31G* basis set for the same reagents show a slightly different picture. They indicate that **7** is 15 kcal/mol less stable than the free reagents. Compound **8** is 9 kcal/mol more stable than **7**, but 6 kcal/mol less stable than the free reagents.

(19) Carey, F. A.; Sundberg, R. J. *Advanced Organic Chemistry Part A: Structure and Mechanisms*, 3rd ed.; Plenum: New York, 1993.
(20) Cotton, F. A.; Wilkinson, G. *Advanced Inorganic Chemistry*, 5th ed.; John Wiley & Sons Inc.: New York, 1988.

Scheme 3. Addition of 1 and 1,4-Diacetylbenzene

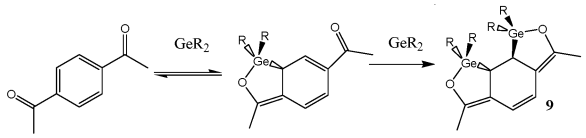

Compound **3** is clearly the most stable though, being 22 kcal/mol more stable than **8**, 31 kcal/mol more stable than **7**, and 16 kcal/mol more stable than the free reagents. Thus although **8** may be a more kinetically favorable product, **3** is the more stable thermodynamic product.

Relationship to Previously Reported Polymerization Chemistry. The competing reactions between **2** and naphthoquinone to form both **5** and polymer are rather enlightening (Scheme 1). Although the cited polymerization reactions were typically performed at −78 °C,[15] our work indicates that polymerization occurs readily at room temperature with less than a 5% yield of **5**. Significantly greater yields of **5** can be generated at room temperature by ensuring that excess germylene is present in solution. Slow addition of naphthoquinone to a solution of **2** over 18 min led to an isolated yield of 30%. The dropwise addition of naphthoquinone to **2** giving greater yields of **5** is consistent with this result. One would expect the high concentration of **2** to increase the rate of the 2:1 addition process and the low concentration of naphthoquinone to slow polymerization. According to Kobayashi et al., the polymer is formed through a biradical mechanism,[21] whereas **5** is presumably formed through a stepwise process similar to **3**, **4**, and **6** (Scheme 2) analogous to the previously reported reaction of **1** with phenones.[18]

Further, it is interesting to note the importance of the quinone in product formation. Although naphthoquinone readily forms a polymer with **2**, the additional aromatic ring in anthraquinone prevents polymerization, instead leading to the exclusive formation of **4**. In both the cases of double activation (**4**) or polymer formation, 2 equiv of germylene must attach to a central anthraquinone. However, only the polymer requires two anthraquinone molecules to bind to each germanium center. This may be the source of a steric influence that distinguishes between double activation and polymerization.

1,4-Diacetylbenzene. Double addition chemistry on a single ring was explored by employing 1,4-diacetylbenzene and germylenes **1** and **2**. Compound **1** reacted with 1,4-diacetylbenzene in a 2:1 ratio, giving two new five-membered rings to form **9** (Scheme 1), although **2** is unreactive toward 1,4-diacetylbenzene. The location of the double bonds after reaction with the first germylene ensures that the second equivalent must attach itself vicinal to the first (Scheme 3). The steric bulk of the germylene enforces the exclusive formation of the *trans* isomer. This material crystallizes readily out of hexane, and a single-crystal X-ray structure was obtained (Figure 4), allowing the presence of three conjugated double bonds to be verified.

The geometrical rigidity imposed upon the dihedral angles of the conjugated triene makes this an interesting test system to benchmark the calculated versus experimental π to π^* transition. The double bonds have dihedral angles of 160.4 (C4−C5−C6−C7) and 169.1 (C2−C3−C4−C5) in the crystal structure. Semiempirical MNDO calculations provided angles of 161.2° and 164.7°, respectively. A pentane solution of **9** gives rise to a UV/vis absorption at 310 nm with an extinction coefficient of 2200 cm^{-1} M^{-1}. This is close to the calculated prediction of an absorbance at 323 nm for the π to π^* transition in **9**. Both the dihedral angles and the UV/vis absorption are similar to those reported for the *cis* and *trans* conjugated trienes 1,1,6,6-tetra-*tert*-butyl-1,3,5-hexatriene.[22] The initial MNDO geometry calculation followed by a single-point B3LYP DFT calculation for energetics resulted in a 5% error to the predicted UV/vis absorption as opposed to the significantly larger errors observed in the HOMO−LUMO gap calculations by Rademacher et al. for similar conjugated polyene systems.[22]

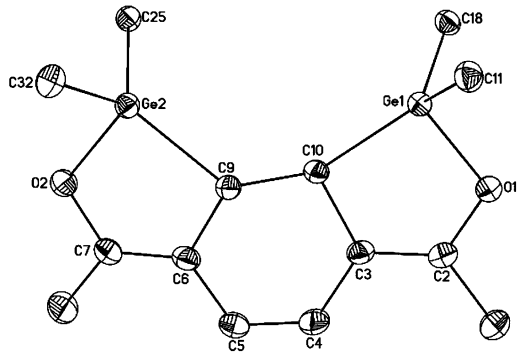

Figure 4. ORTEP of **9** with selected bond lengths (Å), angles (deg), and torsion angle (deg): Ge(1)−O(1) 1.8314(11), Ge(2)−O(2) 1.8335(11), Ge(1)−C(10) 2.0518(15), Ge(2)−C(9) 2.0481(15), C(4)−C(5) 1.344(3), C(9)−C(10) 1.580(2), O(1)−Ge(1)−C(10) 92.08(6), O(2)−Ge(2)−C(9) 92.03(6), Ge(2)−C(9)−C(10) 127.57(10), Ge(1)−C(10)−C(9) 130.02(11) Ge(1)−C(10)−C(9)−Ge(2) 77.91(13).

On the basis of the anthraquinone and naphthoquinone results, it is surprising that **2** does not also react with 1,4-diacetylbenzene. B3LYP DFT calculations using the 6-31G* basis set predict a 40.6 kcal/mol increase in energy for the first activation of **2** into 1,4-diacetylbenzene. A second molecule of **2** adding to 1,4-diacetylbenzene is still 17.9 kcal/mol greater than free **2** and 1,4-diacetylbenzene. The 41 kcal/mol for the first activation of **2** and 1,4-dicacetylbenzene is significantly higher than the 25 and 16 kcal/mol calculated for the first step of the formation of **4** and **5**, respectively. Since the formation of **4** demonstrates that **2** is in equilibrium with the phenone moiety to produce the conjugated triene, the lack of a double addition product suggests that the initial insertion does not occur in this case due to the significantly larger thermodynamic cost of activation of 1,4-diacetylbenzene than the quinones.

1,2-Diacetylbenzene. The importance of the geometry restrictions imparted by the tethered carbonyls in anthraquinone and naphthoquinone cases was explored by reaction with a non-tethered equivalent (1,2-diacetylbenzene). This reaction results in a 1:1 reaction for either germylene **1** or **2** with 1,2-diacetylbenzene to yield

(21) Kobayashi, S.; Iwata, S.; Abe, M.; Shoda, S. *J. Am. Chem. Soc.* **1995**, *117*, 2187−2200.

(22) Rademacher, P.; Kowski, K.; Hopf, H.; Klein, D.; Klein, O.; Suhrada, C. *J. Mol. Struct.* **2001**, *567*, 11−18.

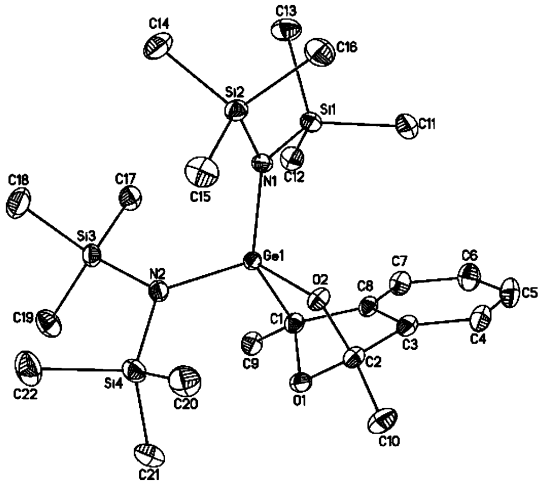

Figure 5. ORTEP of **11** with selected bond lengths (Å) and angles (deg): Ge(1)−O(2) 1.8283(8), Ge(1)−C(1) 2.0229(11), O(1)−C(2) 1.4407(14), O(1)−C(1) 1.4721(14), O(2)−C(2) 1.4361(13), C(1)−C(8) 1.5103(15), C(2)−C(3) 1.5191(16), O(2)−Ge(1)−C(1) 87.99(4), C(2)−O(1)−C(1) 101.99(8), C(2)−O(2)−Ge(1) 106.32(6)

a novel bicyclo compound. The new bicyclo compounds arise through the formation of new germanium−carbon, germanium−oxygen, and carbon−oxygen bonds while consuming the two carbon−oxygen π-bonds (Scheme 1) to give compounds **10** and **11**. The free rotation of the acetyl groups makes this dramatically different reaction pathway possible. A compound with a similar bicyclic ring system, where the germanium is replaced with an oxygen atom, has been previously synthesized. However, this explosive peroxide species was formed from a furan derivative.[23]

Both **10** and **11** are formed quantitatively; no products other than residual starting material and desired product are observable via ^{1}H NMR spectroscopy. Surprisingly, the ^{1}H NMR spectrum signals from the aromatic hydrogens all demonstrate nearly identical shifts. The two different methyl groups also show very similar shifts. However, the ^{13}C NMR spectrum allows one to clearly resolve each of the individual carbons. Both **10** and **11** form needlelike crystals upon slow evaporation from hexanes. A single-crystal X-ray structure of **11** was obtained (Figure 5) that indicated the connectivity shown in Scheme 1.

A simple mechanism can be envisioned for the addition of a germylene to 1,2-diacetylbenzene. Initial coordination of the oxygen to the empty germanium *p* orbital would result in a partial negative charge located on the germanium, similar to our expectations of the initial step in phenone activation. The nucleophilic Ge may then either attack the *ortho* position of the aromatic ring in a manner similar to the phenone activation or the carbonyl carbon. Attack on the carbonyl generates four-coordinate germanium and transfers the formal negative charge to the oxygen. This oxygen can then perform a nucleophilic attack on the carbon of the initial carbonyl, leading to the observed product (Scheme 4). Neither **10** nor **11** shows any sign of equilibrium with free germylene, as no germylene can be trapped upon addition of benzil to these products. If on the other hand

Scheme 4. Stepwise Reaction of Germylene with 1,2-Diacetylbenzene

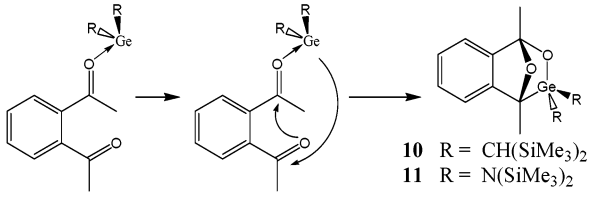

the phenone activation did occur after initial coordination of the germanium and oxygen, then it would be reversible (unless a second equivalent of germylene did indeed coordinate prior to reversion). No indication of either single or double phenone-like activation has ever been observed with 1,2-diacetylbenzene.

Conclusion

The reaction of germylenes with phenones to form trienes has been extended to quinones and diacetyl benzenes. Unlike the phenones, the 1,4-quinones undergo a nonreversible second insertion to form kinetically inert products. The reactions of **2** with the quinones are also the first reported occurrence of amide-substituted germylenes undergoing a [1 + 4] reaction with an aromatic system. These results indicate that an equilibrium with phenones to form the conjugated triene does occur, although the equilibrium for **2** heavily favors the free germylene and phenone. The reaction of **2** with naphthoquinone demonstrated the concentration effects on the copolymerization of the germylene and quinone. Germylene **1** also readily inserts into 1,4-diacetylbenzene, attaching to two adjacent carbons, although **2** does not show this same reactivity. The reaction of 1,2-diacetylbenzene with both germylenes demonstrates the importance in these reactions of having the two carbonyls tethered to each other. Instead of the aromatic activation observed for other phenones a novel bicyclo compound is formed.

Experimental Section

All manipulations were performed using air-free techniques and dry, deoxygenated solvents.[24] All solvents were degassed and dried over sodium benzophenone ketyl. Acetone was dried and degassed over $CaSO_4$. 1,4-Naphthoquinone (Aldrich Chemical) was recrystallized from diethyl ether prior to usage. All other diketones were purchased (Aldrich Chemical) and used without further purification. $Ge[CH(SiMe_3)_3]_2$ (**1**) was prepared via previously reported literature methods.[11] Additional purification steps employed included Soxhlet extraction using hexane and recrystallization from hexane. $Ge[N(SiMe_3)_3]_2$ (**2**) was prepared via previously reported literature methods.[12] ^{1}H NMR and ^{13}C NMR spectra were recorded on a Varian Inova 400 spectrometer at 399.367 and 100.581 MHz, respectively. The spectra were referenced to the residual protons in C_6D_6 at 7.15 ppm or to the natural abundance of ^{13}C in C_6D_6 at 128.00 ppm. IR spectra were obtained as thin films of the products formed by evaporation from solution on NaCl plates on a Perkin-Elmer Spectrum BX. The UV/vis spectra were recorded on a Shimadzu UV160U. High-resolution mass spectra were collected on a VG 70-250-S mass spectrometer using electron impact (70 eV) for ionization.

(23) Saito, I.; Nakata, A.; Matsuura, T. *Tetrahedron Lett.* **1981**, *22*, 1697−1700.

(24) Shriver, D. F.; Drezdon, M. A. *The Manipulation of Air-Sensitive Compounds*, 3rd ed.; Wiley: New York, 1986.

Table 1. Summary of Crystallographic Data for 3, 6, 9, and 11

	3	6	9	11
empirical formula	$C_{42}H_{84}Ge_2O_2Si_8$	$C_{44}H_{88}Ge_2O_2Si_8$	$C_{38}H_{86}Ge_2O_2Si_8$	$C_{22}H_{46}GeN_2O_2Si_4$
fw	990.99	1019.04	944.97	555.56
temperature/K	133(2)	150(2)	150(2)	150(2)
wavelength/Å	0.71073	0.71073	0.71073	0.71073
cryst syst, space group	monoclinic, $P2_1/c$	monoclinic, $C2/c$	triclinic, $P\bar{1}$	triclinic, $P\bar{1}$
unit cell dimens				
a/Å	13.5817(11)	29.688(5)	11.7386(11)	10.1060(9)
α/deg	90	90	105.6510(10)	73.961(10)
b/Å	19.9366(16)	8.9521(15)	14.3887(13)	11.2113(10)
β/deg	105.339(3)	94.900(3)	95.8730(10)	85.505(2)
c/Å	22.2808(18)	21.891(4)	17.8360(16)	13.9057(12)
γ/deg	90	90	111.8570(10)	76.761(2)
volume/Å^3	5818.1(8)	5796.7(17)	2622.1(4)	1473.8(2)
Z, calcd density/ Mg/m^3	4, 1.131	4, 1.168	2, 1.197	2, 1.252
abs coeff/mm^{-1}	1.227	1.233	1.357	1.222
F(000)	2112	2176	1012	592
cryst size/mm	0.26 × 0.40 × 0.46	0.16 × 0.16 × 0.42	0.24 × 0.24 × 0.40	0.44 × 0.36 × 0.34
θ range/deg	2.88−26.56	2.99−28.31	2.83−28.31	3.05−28.31
limiting indices	$-16\le h\le 16$	$-39\le h\le 39$	$-15\le h\le 15$	$-13\le h\le 13$
	$-25\le k\le 25$	$-11\le k\le 11$	$-19\le k\le 18$	$-13\le k\le 14$
	$-24\le l\le 24$	$-29\le l\le 29$	$-18\le l\le 23$	$-18\le l\le 18$
no. of reflns collect/unique	52 043/11 565 [R(int) = 0.0403]	27 291/7095 [R(int) = 0.0398]	26 917/12 827 [R(int) = 0.0257]	16 653/7186 [R(int) = 0.0198]
abs corr	semiempirical from equivalents	semiempirical from equivalents	semiempirical from equivalents	semiempirical from equivalents
refinement method	full-matrix least-squares on F^2	full-matrix least-squares on F^2	full-matrix least-squares on F^2	full-matrix least-squares on F^2
no. of data/restraints/params	11 565/0/507	7095/0/399	12 827/0/477	7186/0/465
goodness-of-fit on F^2	1.064	1.048	1.035	1.057
final R indices [$I>2\sigma(I)$]	R1 = 0.0566	R1 = 0.0371	R1 = 0.0285	R1 = 0.0211
	wR2 = 0.1646	wR2 = 0.0855	wR2 = 0.0717	wR2 = 0.0564
R indices (all data)	R1 = 0.0748	R1 = 0.0495	R1 = 0.0373	R1 = 0.0227
	wR2 = 0.1783	wR2 = 0.0900	wR2 = 0.0755	wR2 = 0.0573
largest diff peak and hole/e Å^{-3}	0.933 and −0.878	0.854 and −0.777	0.448 and −0.345	0.391 and −0.343

Molecular modeling calculations were performed with Spartan '02. For all calculations reported the bis(trimethylsilyl)methyl and bis(trimethylsilyl)amide ligands were approximated by $-CH(SiH_3)_2$ and $-N(SiH_3)_2$, respectively, to reduce the computational requirements of the larger structures. Unless otherwise specified, initial equilibrium geometries were determined using MNDO semiempirical methods. Single-point energy calculations were subsequently performed using B3LYP DFT calculations with the 6-31G* basis set. The resultant energies were within 3 kcal/mol of calculations using exclusively the DFT methods to generate equilibrium geometries. An equilibrium conformer search performed on **7** found a reduction of 0.4 kcal/mol from the conformer determined from the general method used. Although an energetic reduction of a similar magnitude is expected for other calculated compounds, this difference is significantly smaller in magnitude than the difference between compounds and thus should not affect any conclusions.

Reaction of 1 with Anthraquinone (3). Compound **1** (350 mg, 0.895 mmol) and anthraquinone (106 mg, 0.509 mmol) were dissolved in toluene (10 mL), giving a dark red solution. The red color of the solution faded over 12 min to give a pale yellow-brown solution. The solvent was removed in vacuo after 1 h of stirring. The resultant residue was dissolved in pentane (6 mL) and filtered. The tan solid was then washed with pentane (2 × 3 mL). The solvent was removed in vacuo to leave a pale yellow solid (363 mg, 82% yield). ^{1}H NMR spectroscopy showed this material to be **3** with a small amount of excess anthraquinone. The crude **3** was further purified on a silica gel column using a 3% ethyl acetate solution in hexane. A band of yellow material contained pure **3** (260.5 mg, 58.8% yield). Isomer A: ^{1}H NMR (C_6D_6): δ 8.33 (dd, $^3J_{HH}$ = 6.0 Hz, $^4J_{HH}$ = 3.2 Hz, 2 H, Ar−*H*), 7.22 (dd, $^3J_{HH}$ = 6.0, $^4J_{HH}$ = 3.2 Hz, 2 H, Ar−*H*), 6.13 (s, 2 H, C=C−*H*), 3.96 (s, 2 H, Ge−C*H*), 0.36 (s, 18 H, $SiMe_3$), 0.34 (s, 2 H, GeC*H*Si), 0.32 (s, 2 H, GeC*H*Si), 0.24 (s, 18 H, $SiMe_3$), 0.19 (s, 18 H, $SiMe_3$), and 0.09 (s, 18 H, $SiMe_3$). Isomer B: ^{1}H NMR (C_6D_6): δ 8.43 (dd, $^3J_{HH}$ = 6.4 Hz, $^4J_{HH}$ = 3.2 Hz, 2 H, Ar−*H*), 7.29 (dd, $^3J_{HH}$ = 6.4, $^4J_{HH}$ = 3.2 Hz, 2 H, Ar−*H*), 6.52 (s, 2 H, C=C−*H*), 3.64 (s, 2 H, Ge−C*H*), 0.35 (s, 18 H, $SiMe_3$), 0.30 (s, 2H, GeC*H*Si), 0.25 (s, 2 H, GeC*H*Si), 0.20 (s, 36 H, $SiMe_3$), and 0.13 (s, 18 H, $SiMe_3$). Isomer mix: ^{13}C NMR (C_6D_6): δ 147.33 and 147.19 (C=*C*−O); 130.57, 125.10, 124.59, 124.55, 124.45, 124.04, 123.23, 122.80, 120.93, and 118.08 (Ar, *C*=*C*); 36.68 and 36.43 (*C*H−Ge); 15.06, 13.24, 13.08, and 12.49 (Ge*C*HSi); 3.81, 3.72, 3.65, 3.48, 3.35, and 3.24 ($SiMe_3$). IR: No Ge−H or C=O. EI/MS: $[M/Z]^+$= 992.3058 amu. Anal. Calcd for $C_{42}H_{84}GeO_2Si_8$: C, 50.90; H, 8.54. Found: C, 50.63; H, 8.82.

Structure Determination of 3. Colorless, irregular crystals of **3** were grown from a benzene solution at 25 °C. A crystal of dimensions 0.46 × 0.40 × 0.26 mm was cut from a larger mass and mounted on a standard Bruker SMART CCD-based X-ray diffractometer equipped with a LT-2 low-temperature device and normal focus Mo-target X-ray tube (λ = 0.71073 A) operated at 2000 W power (50 kV, 40 mA). The X-ray intensities were measured at 133(2) K; the detector was placed at a distance 4.959 cm from the crystal. A total of 2253 frames were collected with a scan width of 0.3° in ω and ϕ with an exposure time of 30 s/frame. The frames were integrated with the Bruker SAINT[25] software package with a narrow frame algorithm. The integration of the data yielded a total of 52 043 reflections to a maximum 2θ value of 53.11°, of which 11 906 were independent and 9114 were greater than $2\sigma(I)$. The final cell constants (Table 1) were based on the *xyz* centroids of 6376 reflections above $10\sigma(I)$. Analysis of the data showed negligible decay during data collection; the data were processed with SADABS[26] and corrected for absorption. The structure was

(25) *Saint Plus* v. 6.02; Bruker Analytical X-ray: Madison, WI, 1999.
(26) Sheldrick, G. M. *SADABS*, Program for Empirical Absorption correction of Area Detector Data; University of Gottingen: Gottingen, Germany, 1996.

solved and refined with the Bruker SHELXTL[27] software package. All non-hydrogen atoms were refined anisotropically with the hydrogen placed in idealized positions. The compound appears to crystallize as a mixture of *S* and *R* isomers (at C10 and C13). The best fit for the *S*/*R* ratio based upon crystallographic refinement of partial occupancies is 0.65(2)/0.35(2) for C10 and 0.81(2)/0.19(2) for C13. However, we were unable to rationalize partial occupancies with the isomer ratios obtained from the ^{1}H NMR data. Additional details are presented in Table 1 and are given as Supporting Information as a CIF file.

Reaction of 2 with Anthraquinone (4). Anthraquinone (40 mg, 0.19 mmol) and **2** (150 mg, 0.381 mmol) were dissolved in benzene (6 mL) with stirring to produce a bright red solution. This red color slowly faded in intensity for over 12 min to result in a light yellow solution. The solution was stirred for a total of 120 min to ensure complete reaction, before the solvent was removed in vacuo. The resultant yellow residue was dissolved in hexane and filtered through a Whatman 0.25 μm syringe top filter. Slow evaporation of the filtrate yielded **4** as polycrystalline material. The crystals were dried in vacuo to yield analytically pure **4** (176 mg, 93% yield). Isomer A: ^{1}H NMR (C_6D_6): δ 8.42 (dd, $^3J_{HH}$ = 6.0 Hz, $^4J_{HH}$ = 3.2 Hz, 2 H, Ar−*H*), 7.29 (dd, $^3J_{HH}$ = 6.4, $^4J_{HH}$ = 3.2 Hz, 2 H, Ar−*H*), 6.49 (d, $^3J_{HH}$ = 1.6 Hz, 2 H, C═C−*H*), 3.61 (d, $^3J_{HH}$ = 1.2 Hz, 2 H, Ge−C*H*) 0.39 (s, 36 H, $SiMe_3$), 0.24 (s, 36 H, $SiMe_3$). Isomer B: ^{1}H NMR (C_6D_6): δ 8.34 (dd, $^3J_{HH}$ = 6.4 Hz, $^4J_{HH}$ = 3.2 Hz, 2 H, Ar−*H*), 7.22 (dd, $^3J_{HH}$ = 6.0, $^4J_{HH}$ = 3.2 Hz, 2 H, Ar−*H*), 6.12 (s, 2 H, C═C−*H*), 3.82 (s, 2 H, Ge−C*H*) 0.42 (s, 36 H, $SiMe_3$), 0.22 (s, 36 H, $SiMe_3$). Isomer mix: ^{13}C NMR (C_6D_6): δ 145.93 and 145.65 (C═*C*−O); 130.10, 124.05, 124.95, 124.84, 124.51, 124.31, 123.43, 122.92, 119.45, and 116.34 (Ar, *C*═*C*); 38.90 and 36.87 (*C*H−Ge); 5.82, 5.53, 5.46, and 5.21 ($SiMe_3$). IR: No Ge−H or C═O. Anal. Calcd for $C_{38}H_{80}N_4GeO_2Si_8$: C, 45.87; H, 8.10; N, 5.63. Found: C, 45.62; H, 8.34; N, 5.26.

Reaction of 2 with 1,4-Naphthoquinone (5). Compound **2** (200 mg, 0.511 mmol) was dissolved in benzene (20 mL). 1,4-Naphthoquinone (59 mg, 0.26 mmol) was dissolved in 5 mL of benzene and added dropwise over 18 min, with constant agitation, to the germylene solution. The solution was stirred for an additional 20 min to ensure complete reaction and the solvent removed in vacuo to give a pale yellow solid. Acetone (5 mL) was distilled into the flask and allowed to dissolve any soluble material. The solution was then filtered through a frit to remove the insoluble polymeric material. The acetone was removed in vacuo and pentane (3 mL) distilled in. A cold pentane recrystallization produced 77 mg of **5** as a light brown solid (30% yield). Although no impurities were identifiable via ^{1}H NMR spectroscopy, a satisfactory elemental analysis was not obtained. Isomer A: ^{1}H NMR (C_6D_6): δ 6.77 (s, 2 H, Ar−*H*), 6.04 (s, 2 H, C═C−*H*), 3.64 (s, 2 H, Ge−C*H*), 0.39 (s, 36 H, $SiMe_3$), and 0.26 (s, 36 H, $SiMe_3$). Isomer B: ^{1}H NMR (C_6D_6): δ 6.66 (s, 2 H, Ar−*H*), 6.04 (s, 2 H, C═C−*H*), 3.42 (s, 2 H, Ge−C*H*), 0.36 (s, 36 H, $SiMe_3$), and 0.28 (s, 36 H, $SiMe_3$). Isomer mix: ^{13}C NMR (C_6D_6): δ 150.43, 150.05, 129.91, 126.35, 124.56, and 123.70 (Ar); 113.52 and 112.09 (*C*═C); 38.01 and 36.05 (Ge−*C*); 5.82, 5.51, 5.36, and 5.11 ($SiMe_3$). IR: No Ge−H or C═O. EI/MS: $[M/Z]^+$ = 946.2710 amu.

Reaction of 1 with 1,4-Naphthoquinone (6). Naphthoquinone etherate (82 mg, 0.36 mmol) and **1** (300 mg, 0.767 mmol) were dissolved in benzene (12 mL). The solution turned green immediately upon stirring. The solution was stirred for 180 min, then the solvent was removed in vacuo. The 280 mg of this green-gray residue was isolated as crude product (78% yield). The crude material is 90% pure on the basis of ^{1}H NMR spectroscopy. The impurity is naphthoquinone. Crude material (173 mg) was then dissolved in pentane (6 mL) and filtered to remove a green-blue solid. The solution was reduced to approximately 2 mL in volume and cooled to −78 °C and then filtered at −78 °C to give a mixture of white and pale blue solid. A second −78 °C recrystallization of this mixture yielded 5 mg (3% yield) of analytically pure white material. Isomer A: ^{1}H NMR (C_6D_6): δ 6.72 (s, 2 H, Ar−*H*), 6.45 (s, 2 H, C═C−*H*), 3.78 (s, 2 H, Ge−C*H*), 0.25 (s, 2 H, GeC*H*Si), 0.22 (s, 36 H, $SiMe_3$), 0.20 (s, 18 H, $SiMe_3$), 0.17 (s, 18 H, $SiMe_3$), and 0.07 (s, 2 H, GeC*H*Si). Isomer B: ^{1}H NMR (C_6D_6): δ 6.60 (s, 2 H, Ar−*H*), 6.05 (s, 2 H, C═C−*H*), 3.43 (s, 2 H, Ge−C*H*), 0.34 (s, 18 H, $SiMe_3$), 0.33 (s, 18 H, $SiMe_3$), 0.27 (s, 2 H, GeC*H*Si), 0.23 (s, 18 H, $SiMe_3$) 0.21 (s, 2 H, GeC*H*Si), and 0.13 (s, 18 H, $SiMe_3$). Isomer mix: ^{13}C NMR (125.71 MHz, C_6D_6): δ 152.22 and 151.82 (C═*C*−O); 130.31, 128.29, 125.13, 125.08, 112.56, and 111.43 (Ar, *C*═*C*); 36.12 and 36.13 (*C*H−Ge); 14.81, 12.94, 12.86, and 12.43 (Ge*C*HSi); 3.86, 3.71, 3.64, 3.47, 3.45, 3.41, 3.35, and 3.22 ($SiMe_3$). IR: No Ge−H or C═O. Anal. Calcd for $C_{44}H_{88}Ge_2O_2Si_8$: C, 51.86; H, 8.70. Found: C, 52.01; H, 8.38.

Structure Determination of 6. Colorless needles of **6** were grown from a benzene solution at 25 °C. A crystal of dimensions 0.42 × 0.16 × 0.16 mm was cut from a larger needle and mounted similar to **3**. The X-ray intensities were measured at 150(2) K; the detector was placed at a distance 4.959 cm from the crystal. A total of 2068 frames were collected with a scan width of 0.3° in ω and ϕ with an exposure time of 30 s/frame. The frames were integrated with the Bruker SAINT[25] software package with a narrow frame algorithm. The integration of the data yielded a total of 27 291 reflections to a maximum 2θ value of 56.66°, of which 17 442 were independent and 6027 were greater than $2\sigma(I)$. The final cell constants (Table 1) were based on the *xyz* centroids of 5877 reflections above $10\sigma(I)$. Analysis of the data showed negligible decay during data collection; the data were processed with SADABS[26] and corrected for absorption. The structure was solved and refined with the Bruker SHELXTL[27] software package, using the space group *C*2/*c* with $Z = 4$ for the formula $C_{38}H_{82}O_2Si_8Ge_2 \cdot C_6H_6$. All non-hydrogen atoms were refined anisotropically with the hydrogen placed in a mixture of idealized and refined positions. The compound crystallizes as a 50/50 mixture of the *R* and *S* isomers related by a crystallographic inversion center. The benzene lattice solvate occupies an inversion center in the lattice. Additional details are presented in Table 1 and are given as Supporting Information as a CIF file.

Reaction of 1 with 1,4-Diacetylbenzene (9). 1,4-Diacetylbenzene (21 mg, 0.13 mmol) and **1** (100 mg, 0.26 mmol) were placed in a glass bomb and dissolved in hexane (6 mL). The solution immediately became a pale yellow color. After stirring the solution for 18 h, the volatiles were removed in vacuo to afford a yellowish residue. The residue was dissolved in benzene and filtered through a 15 mm column of dry Celite. Slow evaporation of the filtrate yielded analytically pure material (97 mg, 80.8% yield). ^{1}H NMR (C_6D_6): δ 6.14 (s, 2 H, C═C*H*), 3.21 (s (br), 2 H, Ge−C*H*), 1.91 (s, 6 H, C*H*$_3$) 0.57 (s, 2 H, GeC*H*Si), 0.36 (s, 18 H, $SiMe_3$), 0.35 (s, 18 H, $SiMe_3$), 0.34 (s, 18 H, $SiMe_3$), 0.32 (s, 18 H, $SiMe_3$). ^{13}C NMR (125.73 MHz, C_6D_6): δ 151.28 (C═*C*−O); 128.29 and 118.11 (*C*═C); 26.27 (*C*H); 17.28 (*C*H$_3$); 13.53 and 14.09 (Ge*C*HSi); 5.56, 5.13, 5.01, and 4.29 ($SiMe_3$). IR: No Ge−H or C═O. UV/vis λ_{max}: 310 nm, ϵ = 2200 cm^{-1} M^{-1}. EI/MS $[M/Z]^+$ = 944.3061. Anal. Calcd for $C_{38}H_{86}Ge_2O_2Si_8$: C, 48.30; H, 9.17. Found: C, 48.22; H, 9.35.

Structure Determination of 9. Colorless blocks of **9** were grown from a toluene solution at −20 °C. A crystal of dimensions 0.40 × 0.24 × 0.24 mm was mounted similar to **3**. The X-ray intensities were measured at 150(2) K; the detector was placed at a distance 4.954 cm from the crystal. A total of 2028 frames were collected with a scan width of 0.3° in ω and ϕ with an exposure time of 25 s/frame. The frames were integrated with the Bruker SAINT[25] software package with a narrow frame algorithm. The integration of the data yielded a total of 26 917 reflections to a maximum 2θ value of 56.62°,

(27) *SHELXTL*, v. 5.10; Bruker Analytical X-ray: Madison, WI, 1997.

of which 12 827 were independent and 10 940 were greater than $2\sigma(I)$. The final cell constants (Table 1) were based on the *xyz* centroids of 7873 reflections above $10\sigma(I)$. Analysis of the data showed negligible decay during data collection; the data were processed with SADABS[26] and corrected for absorption. The structure was solved and refined with the Bruker SHELXTL[27] software package. All non-hydrogen atoms were refined anisotropically with the hydrogens placed in idealized positions. Additional details are presented in Table 1 and are given as Supporting Information in a CIF file.

Reaction of 1 with 1,2-Diacetylbenzene (10). 1,2-Diacetylbenzene (103 mg, 0.639 mmol) and **1** (250 mg, 0.639 mmol) were dissolved in hexane (10 mL). Within 30 min, the yellow color of **1** had faded. After stirring for 24 h, the volatiles were removed in vacuo, leaving an off-white residue. This material was suspended in a small amount of CH_3CN; the solvent was decanted to remove the residual 1,2-diacetylbenzene. Analytically pure crystals were obtained by redissolving in a minimal amount of hexane and slow evaporation of the solvent to yield 289 mg (82%) of **10** as white crystals. ^{1}H NMR (C_6D_6): δ 7.00 (m, 4 H, Ar−*H*), 1.95 (s, 3 H, C*H*$_3$), 1.94 (s, 3 H, C*H*$_3$) 0.49 (s, 9 H, $SiMe_3$), 0.40 (s, 1 H, Ge−C*H*−Si), 0.30 (s, 9 H, $SiMe_3$), 0.15 (s, 9 H, $SiMe_3$) 0.08 (s, 1 H, Ge−C*H*−Si), and −0.07 (s, 9 H, $SiMe_3$). ^{13}C NMR (C_6D_6): δ 148.90, 145.72, 126.63, 126.44, 120.88, 119.02 (Ar), 106.11, 85.89 (*C*−O), 20.88, 18.32 (CH_3), 14.09 and 12.71 (Ge*C*HSi), 4.61, 4.19, 3.98, and 3.90 ($SiMe_3$). IR: No Ge−H or C═O. Anal. Calcd for $C_{24}H_{48}GeO_2Si_4$: C, 52.07; H, 8.74. Found: C, 52.05; H, 8.58.

Reaction of 2 with 1,2-Diacetylbenzene (11). 1,2-Diacetylbenzene (24 mg, 0.15 mmol) and **2** (60 mg, 0.15 mmol) were dissolved in benzene (5 mL). The solution was stirred for 18 h before the volatiles were removed in vacuo. The tan solid was then dissolved in hexane (2 mL) and filtered using a Whatman 0.02 μm pore syringe top filter. Slow evaporation of the filtrate yielded analytically pure, off-white crystals of **11** (65 mg, 77% yield). ^{1}H NMR (C_6D_6): δ 6.95 (m, 4 H, Ar−*H*), 1.91 (s, 3 H, C*H*$_3$), 1.84 (s, 3 H, C*H*$_3$) 0.50 (s, 18 H, $SiMe_3$), 0.09 (s (br), 18 H, $SiMe_3$). ^{13}C NMR (C_6D_6): δ 149.33, 144.14, 127.09, 126.56, 121.57, and 119.43 (Ar), 106.38 (O−*C*−O), 86.96 (O−*C*−Ge), 21.37, 16.66 (*C*H$_3$), 6.48 and 5.43 ($SiMe_3$). IR: No Ge−H or C═O. Anal. Calcd for $C_{22}H_{46}N_2GeO_2Si_4$: C, 47.56; H, 8.35; N, 5.04. Found: C, 47.51; H, 8.21; N, 5.15.

Structure Determination of 11. Colorless blocks of **11** were grown from a benzene-d_6 solution at 25 °C. A crystal of dimensions 0.44 × 0.36 × 0.34 mm was cut from a larger mass and mounted similar to **3**. The X-ray intensities were measured at 150(2) K; the detector was placed at a distance 4.954 cm from the crystal. A total of 2448 frames were collected with a scan width of 0.3° in ω and ϕ with an exposure time of 20 s/frame. The frames were integrated with the Bruker SAINT[25] software package with a narrow frame algorithm. The integration of the data yielded a total of 16 653 reflections to a maximum 2θ value of 56.69°, of which 7186 were independent and 6799 were greater than $2\sigma(I)$. The final cell constants (Table 1) were based on the *xyz* centroids of 6550 reflections above $10\sigma(I)$. Analysis of the data showed negligible decay during data collection; the data were processed with SADABS[26] and corrected for absorption. The structure was solved and refined with the Bruker SHELXTL[27] software package. All non-hydrogen atoms were refined anisotropically with the hydrogen atoms located on a difference Fourier map and allowed to refine isotropically. Additional details are presented in Table 1 and are given as Supporting Information as a CIF file.

Sample Benzil Trapping Experiment. Benzil (11 mg, 0.052 mmol) was added to **4** (10 mg, 0.10 mmol) in benzene-d_6 (0.7 mL). The solution was monitored via ^{1}H NMR spectroscopy. After 10 days, no trapped germylene was detectable by ^{1}H NMR spectroscopy. The solution was then placed in a 55 °C oil bath for 24 h. Still no trapped germylene was observed by ^{1}H NMR spectroscopy.

UV/Vis Spectroscopy Experiments. Stock solutions of the germylene and quinones were used for all experiments. A sample experiment is described. In an air-free atmosphere, 2 mL of a 5 mM anthraquinone solution in THF was placed in a cuvette, and 5 mL of a 4 mM solution of **1** was placed in an attached flask. The apparatus was sealed from the atmosphere and a spectrum of the anthraquinone acquired. The two solutions were mixed, and immediately a series of spectra were acquired during the duration of the color change.

Quenching the reaction with benzil was accomplished in the same manner, but after mixing the two solutions and acquiring an initial UV/vis spectrum, the solution was exposed to the ambient atmosphere, a solution of benzil (30 mg, 0.16 mmol) in dry THF (0.4 mL) was introduced, and the solution was remixed to ensure homogeneity.

Acknowledgment. We thank the Petroleum Research Fund for financial support of this project.

Supporting Information Available: X-ray crystallographic data for compounds **3**, **6**, **9**, and **11**. This material is available free of charge via the Internet at http://pubs.acs.org. Crystallographic data have also been deposited with the Cambridge Crystallographic Data Centre. Copies of this information may be obtained free of charge from the CCDC, 12 Union Rd, Cambridge CB2 1EZ, U.K. (fax: +44 1223 336033; e-mail: deposit@cam.ac.uk or http://www.ccdc.cam.ac.uk).

OM0302589